

Automated X-ray Focusing Using Kirkpatrick-Baez Bimorph Mirrors

Derek W. Yoder^a, Sergey Stepanov^a, Riccardo Signorato^b, Robert F. Fischetti^a

^aGM/CA-CAT, Biosciences Division, Argonne National Laboratory, Argonne, IL 60439, USA

^bACCEL Instruments, GmbH, Bergisch Gladbach, Germany

Four bimorph focusing mirrors have been installed on two insertion device beamlines operated by GM/CA-CAT at the Advanced Photon Source. Using the bimorph functionality, the optics can be shaped to deliver an X-ray beam with the desired focal properties. This process is complex due to the many degrees of freedom. To deal with this multi-dimensional challenge, a matrix approach is applied to predict the optimum voltages. These methods require information on the voltage dependence of the slope error of the mirrors. GM/CA has employed a number of techniques for measuring these data and has developed the controls needed for automated collection and analysis. Focused beams of approximately 25 microns by 70 microns, which retain a pseudo-Gaussian shape off focus, are routinely used for challenging macromolecular crystallographic data collections, e.g. to obtain data on large unit cells or to condition the full beam for our minibeam ($5 \times 5 \mu\text{m}^2$) apparatus.

Keywords: mirror, bimorph, automation, crystallography

PACS: 87.64.Bx, 07.85.Qe

1. Introduction

The benefits of using bimorph technology in X-ray focusing mirrors are now well documented and understood [1-3]. The bimorph capability may be used to shape the mirror to focus the X-ray beam, minimize the slope error, or correct aberrations in the X-ray wavefront. At the General Medicine and Cancer Institutes Collaborative Access Team (GM/CA-CAT, Sector 23) of the Advanced Photon Source, we have installed vertical and horizontal focusing bimorph mirrors on both insertion device beamlines (23-ID-B and 23-ID-D) [4]. These mirrors were constructed by SESO (Aix en Provence, France). The mirror electronics [5] (voltage controllers and focusing drivers) were developed by Elettra (Trieste, Italy). ACCEL (Bergisch Gladbach, Germany) was responsible for physical integration of the mirrors into the beamlines. Here, we present results obtained with these mirrors and describe the software controls implemented to automate the focusing process.

The mirror construction has been described previously [3]. Briefly, the mirrors resemble a sandwich with long fused-silica plates surrounding two segmented layers of a piezoelectric ceramic material. The silica surfaces are polished and may also be coated to achieve the desired reflective properties. At GM/CA, we use uncoated silica ($E_{\text{crit}}\theta \sim 30 \text{ keV}\cdot\text{mrad}$, where ' E_{crit} ' is the critical energy at ' θ ', the angle of X-ray incidence), as well as rhodium ($E_{\text{crit}}\theta \sim 62 \text{ keV}\cdot\text{mrad}$) and platinum ($E_{\text{crit}}\theta \sim 80 \text{ keV}\cdot\text{mrad}$) coatings. Driving electrodes are deposited at the boundary of the piezoelectric layers, and pairs of common electrodes are deposited at the piezoelectric/silica boundaries. To accept the full cone of the photon beam, GM/CA uses horizontal mirrors that are 1050 mm long (with 14 electrodes), and vertical mirrors that are 600 mm long (with 16 electrodes). The stable application of voltages to the electrodes is provided by a controller accessible via both a web interface and EPICS, which GM/CA uses for beamline control. The layout of the optical components on the two beamlines is qualitatively similar. The approximate demagnification ratios are 6.0:1 and 6.9:1 (horizontal and vertical, respectively) at 23-ID-B and 10.4:1 and 12.5:1 at 23-ID-D.

2. Focal Technique and Characterization Methods

Beam focusing requires using the bimorph capability to correct the slope error of each mirror segment to direct the reflected beam from that segment to the focal position. The ability to refine multiple degrees of freedom and to perform this work *in situ* is the primary advantage between bimorph mirrors and more “traditional” mirrors. In practice, this adjustment is accomplished by illuminating a small portion of the mirror with an X-ray “beamlet”, measuring the centroid of the reflected beamlet at the focal position, and adjusting the driving voltage as necessary. Centroid positions may be determined by a number of methods including: performing a slit scan; using a position sensitive detector; or by analyzing the beam image on a scintillator crystal. A schematic of this process is shown in Fig. 1.

Although individual voltages may be refined iteratively, this process is cumbersome. Therefore, we employ the matrix inversion technique described previously [3]. This technique uses a matrix of data describing the response of each segment (as determined by the motion of the beamlet centroids) to voltage pulses applied sequentially to each electrode along the length of the mirror. This “interaction matrix” is then inverted and applied to the error vector describing the existing mirror state. The result is the voltage correction vector needed to focus the mirror. The software which performs these calculations is included with the mirror controller and is accessible through an embedded web server.

Despite making the focusing process significantly more efficient, this technique is still data intensive. It requires slope error information (in the form of beamline centroids) from each of the mirror segments, and generally the segments are oversampled. This information must be gathered for an initial voltage state and for each of the voltage pulses applied. In total, the matrix may easily surpass four hundred elements and could approach one thousand. Because of the quantity of data required and because of the repetitive nature of its collection, we have automated the focal process.

3. Automation

A variety of controls have been implemented at GM/CA-CAT [6] to automate the entire focusing process. A Tcl/Tk GUI (Fig. 2) provides convenient access to these controls. One library of Perl scripts is responsible for collecting the matrix data described above, and all relevant beamline components (e.g. motors, attenuators, and counting electronics) are controlled. When the centroid information is gathered with slit profiling, we employ “on-the-fly” hardware synchronized scanning [7] to measure individual beamlet profiles in as little as four seconds. A second library controls communication with the mirror controller via both HTTP and EPICS: while the controller provides voltage I/O through both EPICS and HTTP, the “interaction matrix” is only accessible via HTTP. In addition to these controls, a number of related utilities have been developed including voltage backup/restore functionality, controlling the refresh rate for the mirror PVs, and EPICS MEDM screens for GUI interaction with the controller. Additionally, we have automated mechanical mirror alignment – a non-focal operation.

4. Focal Results and Conclusion

The matrix focal technique efficiently produces a clean beam profile in a single step. Figure 3 shows the full beam profile before (left) and after (right) applying the voltage correction vector. The focal size ($V \times H$) is typically $25 \times 70 \mu\text{m}^2$ and $25 \times 120 \mu\text{m}^2$ FWHM at 23-ID-D and 23-ID-B, respectively. The horizontal size reflects the demagnification ratio of the given beamline, while the vertical is dominated by the slope error of the mirror ($\sim 1 \mu\text{rad}$). Furthermore, a near Gaussian profile is maintained even at distances of nearly one meter from the focal location. These beams have been used in a variety of challenging crystallographic data acquisitions. Gan, Johnson and coworkers [8] have determined the structure of the HK97 virus capsid (cell dimensions of $1010 \times 1010 \times 732 \text{ \AA}^3$) using a beam focused at the detector

position, 680 mm downstream of the crystal. A clean profile was maintained at the crystal location. Also, these beams have been used in conjunction with GM/CA's minibeam apparatus to deliver spots as small as $5 \times 5 \mu\text{m}^2$ for use with particularly small crystals. A well focused beam is essential to maintaining low noise levels in the intensity. A number of difficult structures have now been determined by using this apparatus exclusively [9, 10].

Acknowledgements

GM/CA-CAT has been funded with Federal funds from the National Cancer Institute (Y1-CO-1020) and the National Institute of General Medical Science (Y1-GM-1104). Use of the Advanced Photon Source was supported by the U.S. Department of Energy, Basic Energy Sciences, Office of Science, under contract No. DE-AC02-06CH11357.

References

- [1] R. Signorato, *Synchrotron Radiation Instrumentation* 705 (2004) 812.
- [2] R. Signorato, D. Hausermann, M. Somayazulu, J.F. Carre, *Proceedings of the SPIE - The International Society for Optical Engineering* 5193 (2004) 112.
- [3] R. Signorato, O. Hignette, J. Goulon, *Journal of Synchrotron Radiation* 5 (1998) 797.
- [4] R.F. Fischetti, et al., *Synchrotron Radiation Instrumentation* 879 (2007) 754.
- [5] M. Cautero, G. Cautero, B. Krastanov, F. Bille, R. Borghes, L. Iviani, D. Cocco, G. Sostero, R. Signorato, *Synchrotron Radiation Instrumentation* 879 (2007) 683.
- [6] S. Stepanov, O. Makarov, A. Urakhchin, U. Schwabe, C. Venkataraman, R. Pugliese, *Architecture and highlights of control system for GM/CA-CAT macromolecular crystallography beamlines in: NOBUGS-2004 Conference Program & Abstracts, Paul Scherrer Institute, Switzerland, 2004.*
- [7] S. Stepanov, O. Makarov, E. Kondrashkina, B. Deriy, D.W. Yoder, S. Devarapalli, S. Corcoran, R.F. Fischetti, *Hardware-synchronized on-the-fly scans at GM/CA-CAT beamlines in: NOBUGS-2006 Conference Program & Abstracts, Lawrence Berkeley National Laboratory, Berkeley, CA, 2006.*
- [8] L. Gan, J.A. Speir, J.F. Conway, G. Lander, N.Q. Cheng, B.A. Firek, R.W. Hendrix, R.L. Duda, L. Liljas, J.E. Johnson, *Structure* 14 (2006) 1655.
- [9] V. Cherezov, et al., *Science* 318 (2007) 1258.
- [10] S.G.F. Rasmussen, et al., *Nature* 450 (2007) 383.

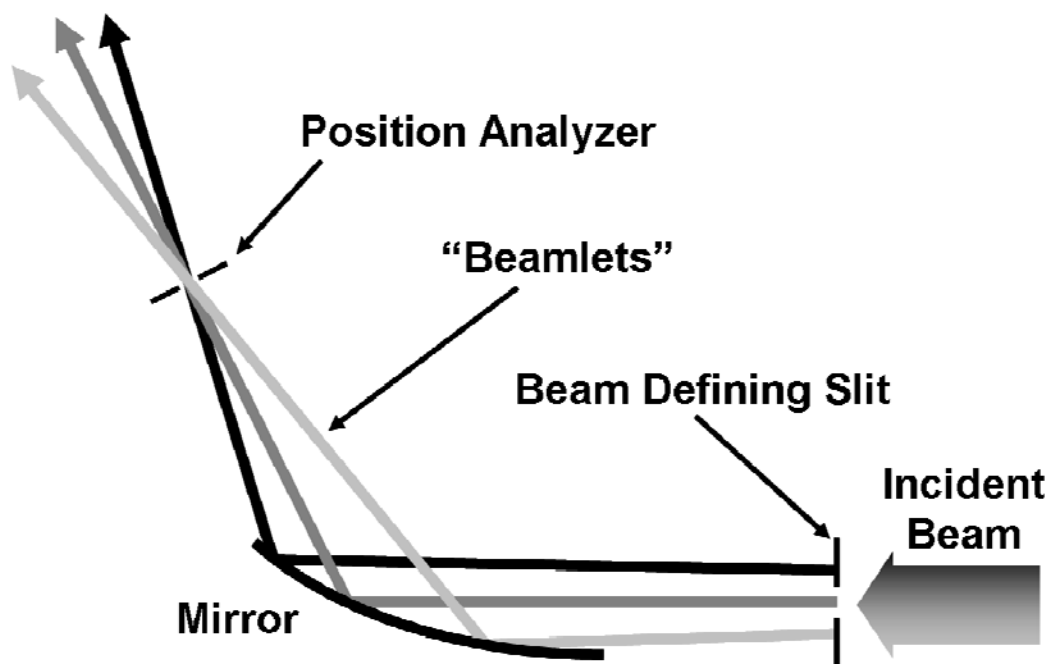


Figure 1 – A schematic representation of the technique for assembling the interaction matrix.

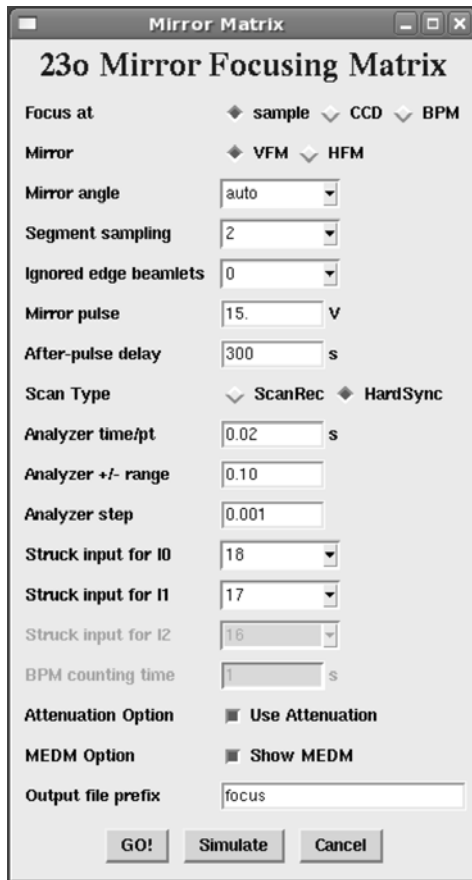


Figure 2 – The tcl/tk GUI used for setting up automated collection of the matrix data.

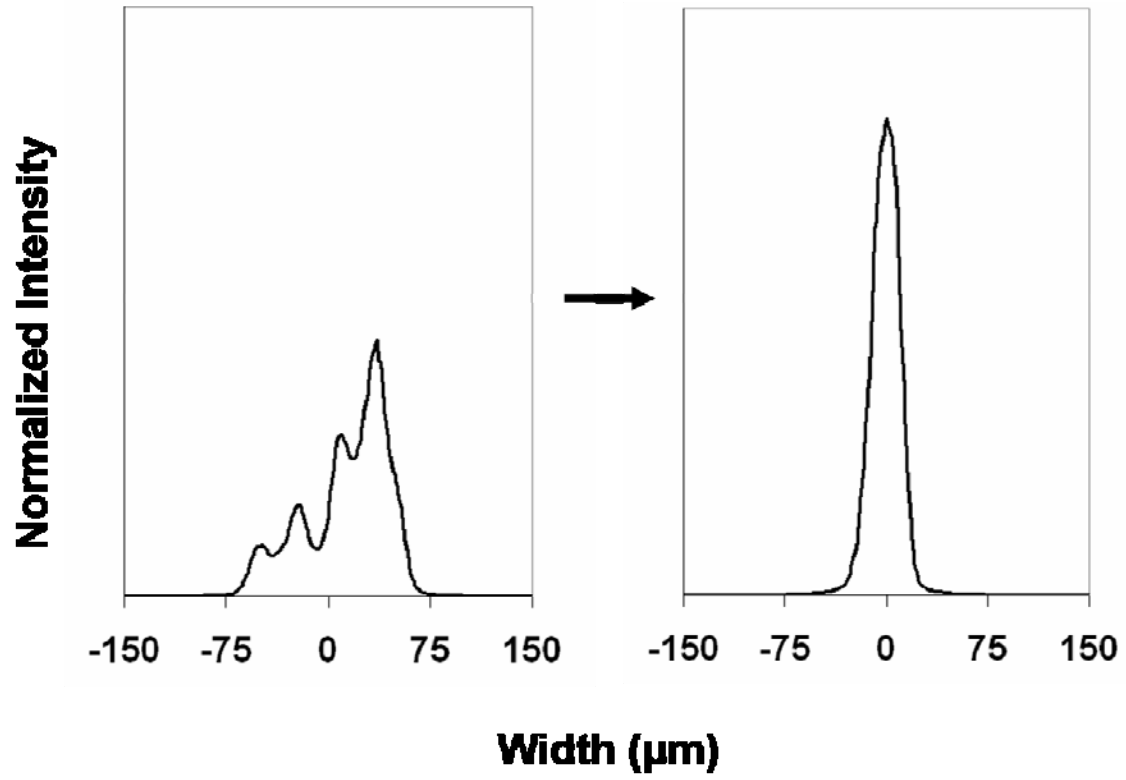


Figure 3 – The matrix inversion technique efficiently focuses the beam in just a single step.